



Title	Synergistic enhancement of biomass and lipid productivity in Chlorella sorokiniana co-cultured with engineered vitamin-producing <i>Escherichia coli</i>
Author(s)	Tong, C. Y.; Tomita, Hiroya; Miyazaki, Kentaro et al.
Citation	Algal Research. 2026, 93, p. 104442
Version Type	VoR
URL	https://hdl.handle.net/11094/103573
rights	This article is licensed under a Creative Commons Attribution-NonCommercial 4.0 International License.
Note	

The University of Osaka Institutional Knowledge Archive : OUKA

<https://ir.library.osaka-u.ac.jp/>

The University of Osaka



Synergistic enhancement of biomass and lipid productivity in *Chlorella sorokiniana* co-cultured with engineered vitamin-producing *Escherichia coli*



C.Y. Tong ^{a,b}, Hiroya Tomita ^b, Kentaro Miyazaki ^b, C.J.C. Derek ^a, Kohsuke Honda ^{b,*}

^a School of Chemical Engineering, Engineering Campus, Universiti Sains Malaysia, Nibong Tebal, 14300, Penang, Malaysia

^b International Center for Biotechnology, The University of Osaka, 2-1 Yamada-oka, Suita, Osaka, 565-0871, Japan

ARTICLE INFO

Keywords:

Biodiesel production
Chlorella sorokiniana
 Metabolic engineering
 Microalgal-bacterial co-culture
 Vitamin biosynthesis genes

ABSTRACT

Recognizing that approximately 50–70 % of green microalgae are vitamin auxotrophs, co-cultivation with vitamin-producing bacteria presents a promising strategy in boosting the microalgal growth, yet natural partnerships often lack efficiency. To address this research gap, this study establishes a synthetic vitamin-based mutualism by metabolically engineered *Escherichia coli* BL21(DE3) to enhanced vitamin production. Specifically, riboflavin biosynthetic *zwf-fbp* genes, cobalamin biosynthetic *cobU-cobC* genes, and biotin biosynthetic *bioF-bioD* genes were cloned in three compatible T7 promoter-based expression plasmids and were co-introduced into the bacterial host strain, yielding a recombinant strain RS04. *Chlorella sorokiniana* was then co-cultured with RS04 and examined for cell growth and lipid accumulation. Results showed at least a four-fold increase in algal growth as indicated by Chl-*a* fluorescence intensity (a resulting microalgal-to-bacterial dry weight ratio of 6.2), at Day 7, compared to the controls. At the early co-cultivation phase, microalgae appeared to sustain bacterial viability, exhibiting a bacterial growth rescue effect from Day 14–28. Based on the observed vitamin levels in the cultivation medium and preliminary interpretation, a potential sequential vitamin assimilation model was proposed: biotin (initial uptake) → cobalamin (consistent need) → riboflavin (slowest). In terms of biodiesel properties, this consortium enhanced cold weather performance (~18 °C cloud point; 4.8 mm² s⁻¹ kinematic viscosity) and fuel efficiency (~40 MJ kg⁻¹). This study demonstrated that microalgae produce lipids in a short time under a highly stable co-cultivation system.

1. Introduction

Microalgae, a 3rd generation biofuel feedstock, has become a nationwide interest due to its strong survival adaptability, which enables cultivation in diverse and non-arable environments, thereby minimizing competition for agricultural land [1]. Since there were significant strides in researching microalgal biodiesel, several species such as *Chlorella* sp., *Nannochloropsis* sp., *Dunaliella* sp., *Botryococcus* sp., *Desmodesmus* sp., *Neochloris* sp., *Scenedesmus* sp. and *Tetraselmis* sp. have been acknowledged as suitable candidates to produce biodiesel that meets both ASTM D6751 standards and EN14214 standards [2]. While extensive studies have documented methods for producing lipids from microalgae [3–5], fundamental limitations cannot be overcome if biomass productivity remains insufficient to meet supply demands. Monoculture of microalgae usually pose significant challenges due to contamination by other microorganisms, diluted cell density, unstable hydrodynamic stress, and low metabolite concentration [1]. Therefore,

cultivation remains a crucial step in the process from algal growth to lipid biosynthesis and biodiesel refining.

Recently, combining microalgal cultivation with symbiotic bacteria has emerged as a promising approach for biofuel production. One of the objectives of co-cultivation is to mix two or more species in such a way that one strain possesses enzymatic activity that is absent in the other, thereby fostering mutual benefit and synergistic interactions [6]. For instance, both *Pseudomonas composti* cells and their cell-free filtrate promoted increases in biomass yield and lipid content of freshwater *Characium* sp. 46–4, within 7 days of co-cultivation [7]. The highly efficient ammonia-oxidizing bacterial strain FN5 enhanced the biomass and lipid content of *Chlorella pyrenoidosa* by 14.8 % and 13.6 % [8]. A pollutant-tolerant microalga *Desmodesmus* sp. and *Bacillus megaterium* co-culture improved the total lipid content by approximately 45.9 % as compared to the blank control while treating raw dairy manure wastewater [9]. However, most of these studies primarily focused on biochemical engineering strategies, such as optimizing cultivation

* Corresponding author.

E-mail address: honda.kohsuke.icb@osaka-u.ac.jp (K. Honda).

conditions and nutrient limitation to stimulate lipid accumulation, but they lacked meaningful advancements in elucidating the role of bacterial-derived metabolites that contribute to both biomass and lipid productivity enhancement.

Associating with this, the vitamin auxotrophy of microalgae plays a crucial role in the development of cellular biochemistry. A half (156/312 species) of the microalgal species in both fresh and marine aquatic systems are cobalamin-auxotrophs, 23 % (72/312 species) are thiamine-auxotrophs, while 4.8 % (15/312 species) are biotin-auxotrophs [10]. A combination of different vitamins would speed up the algal growth. Since microalgae are incapable of synthesizing most vitamins (such as cobalamin, thiamin, and biotin) de novo, they must acquire vitamins exogenously from co-living organisms such as bacteria. For example, bacterium *Mesorhizobium loti* supplies cobalamin to freshwater alga *Lobomonas rostrata*, while receiving algal photosynthate in return [11]. For bacteria associated with *Chlorella* sp., their predicted functional genes suggested an involvement in the metabolism and biosynthesis of B-complex vitamins, including cobalamin, thiamine, biotin, pyridoxine, and riboflavin [12]. A trace amount of cobalamin (100 ng L⁻¹) improved the biological adsorption of the *Chlorella vulgaris*-*Bacillus licheniformis* consortium. This, in turn, enriched metabolic pathways linked to carbon fixation and the photosynthesis of algal cells, as well as the quorum-sensing pathway that stimulates algal-bacterial interactions [13]. Additionally, riboflavin and lumichrome produced by *Azospirillum brasilense* was found to promote the growth and metabolism of *Chlorella sorokiniana* [14].

Studies have demonstrated the widespread occurrence of vitamin auxotrophy in microalgae, directly providing impetus for future work. Given that bacteria like *E. coli* can synthesize most vitamins de novo with suitable precursors, a potential research approach involves metabolically engineering the bacteria to overproduce essential vitamins and subsequently assessing their impact on algal growth. Previous study used to demonstrate that an addition of 0.62 mg L⁻¹ blend of biotin, cyanocobalamin, and thiamine (in a 1:1:200 ratio) led to a 16 % increase in lipid content of *Scenedesmus* sp., indicating its positive effect on microalgal lipid accumulation [15]. Another separate study depicted the same observation when the measured lipid accumulation in microalgae grown in medium supplemented with additional vitamin (B₁, B₇, B₅, and B₁₂) amount was much higher than the control group [16]. Therefore, in this study, we hypothesized that an engineered bacterial load could elicit a synergistic effect on the growth of *Chlorella sorokiniana*, addressing the challenge of lipid productivity in green microalgae. Species within the genus *Chlorella* was chosen due to its promising resources for biodiesel production, pharmaceutical applications, and wastewater treatment, owing to their remarkable physiological plasticity [17]. In addition, this species was also demonstrated to establish stable consortia with *E. coli* in our previous study [18,19]. Although *C. sorokiniana* is not strictly vitamin auxotrophic, its high compatibility with *E. coli* may create conditional vitamin requirements, leading to further growth stimulation compared with conventional co-culture, via a coupling effect of bacterial presence and vitamin contributions from the engineered bacteria. We contend that a provision of vitamin-enriched substrates by bacteria could augment lipid yield without compromising algal growth. Besides its lipid yields, the biodiesel quality was estimated to meet the biofuel industry's demand. The entire analysis revealed the potential of co-culturing engineered bacteria with specific microalgae, highlighting additional avenues for genetic engineering techniques to cater to specific needs in the future.

2. Materials and methods

2.1. Strains, plasmids, and cultivation conditions

Microalgae, *Chlorella sorokiniana* 211/8 K (Culture Collection of Algae and Protozoa [CCAP], Scotland, UK) was cultivated in BG11 medium and incubated at 25±2°C under cool fluorescent white light

around 120 μmol photon m⁻² s⁻¹. *E. coli* DH5α was used for plasmid construction and cloning, whereas *E. coli* BL21(DE3) was used for overexpression of cloned genes. *E. coli* cells were cultivated in LB medium (Lennox, Nacalai Tesque, Kyoto, Japan) at 37°C. Gene overexpression was performed using plasmids (Merck Millipore, Billerica, MA, USA) with different replication origins and antibiotic resistance: pETDuet-1, pACYCDuet-1, and pCDFDuet-1.

2.2. Gene cloning and construction of recombinants

The metabolic engineering strategies for symbiotic bacteria in this study was adapted from our previous work [18,19], which has successfully identified algal growth-promoting genes and beneficial bacterial-derived metabolites. Building upon the shortlisted genes deemed suitable for overexpression to enhance the biosynthesis of vitamin-based metabolites in *E. coli*, this study focuses specifically on riboflavin, cobalamin, and biotin, which were revealed to promote microalgal growth [18]. Three plasmids with different antibiotic resistance and replication origins were employed to overexpress two key genes responsible for riboflavin, cobalamin, and biotin biosynthesis at two cloning sites in each vector as illustrated in Fig. 1. All the bacterial strains and plasmids used in this work are described in Supplementary data S1. Primers used in this work are listed in Supplementary data S2.

To construct a riboflavin-overproducing plasmid, *zwf* (encoding glucose-6-phosphate 1-dehydrogenase) and *fbp* (encoding fructose-1,6-biphosphatase I) genes were amplified using *zwf*-MCS1-Fwd and *zwf*-MCS1-Rev and *fbp*-MCS2-Fwd and *fbp*-MCS2-Rev primers, respectively. Corresponding vectors were amplified using pET-*fbp*-MCS1-Fwd pET-*fbp*-MCS1-Rev and pET-*fbp*-MCS2-Fwd and pET-*fbp*-MCS2-Rev primers, respectively. Two gene fragments were inserted sequentially into its corresponding cloning site by Gibson assembly (NEBuilder HiFi DNA Assembly Master Mix, New England Biolabs). First, the *fbp* gene was assembled into the MCS2 of the pETDuet-1 vector, followed by the insertion of the *zwf* gene into the MCS1, resulting in a final construct named pETDuet-1-*zwf-fbp*. Similarly, the other two sets of genes: *cobU* (encoding bifunctional adenosylcobalamin biosynthesis protein) and *cobC* (encoding adenosylcobalamin/alpha-ribazole phosphatase), and *bioF* (encoding 7-keto-8-amino pelargonic acid synthase) and *bioD* (encoding desthiobiotin synthase) were cloned into pACYCDuet-1 and pCDFDuet-1 respectively, to yield pACYCDuet-1-*cobU-cobC* and pCDFDuet-1-*bioF-bioD*. Each of these plasmids was transformed into *E. coli* BL21(DE3), resulting in the generation of recombinant strains RS01, RS02, and RS03. In addition, all three plasmids were introduced into a single BL21(DE3) cell to produce the strain RS04.

2.3. Co-cultivation medium preparation and conditions

All the constructed recombinant strains were routinely grown in LB broth or on LB agar plates at 37°C. Where necessary, respective antibiotics were added to a final concentration of 50 μg mL⁻¹. The overnight seed cultures (1 mL) of recombinant strains were used to inoculate 250 mL shake flasks containing 100 mL of LB medium supplemented with appropriate antibiotics and incubated at 37°C in a rotary shaker at 180 rpm until reaching OD₆₀₀ of about 0.6. Then, 0.1 mM isopropyl-β-D-1-thiogalactopyranoside (IPTG) was added to induce expression at 18 °C, and the cells were grown for an additional 18 h. On the other hand, 90 mL one-week-old microalgal cultures were pelleted at 2263 × g for 10 min and the supernatant was discarded. The algal cell pellets were then re-suspended with an equal volume of sterile BG11 medium and subsequently mixed with 90 mL of IPTG-induced bacterial cultures. Such a co-cultivation approach was adapted from our previous optimized findings, utilizing a 1:1 (v/v) ratio of BG11 to bacterial supernatant (consisting of antibiotics) as the co-cultivation medium and a bacteria-to-microalgae inoculum size of 5:1 on a dry weight basis [19].

The mixture was divided among three separate shaking flasks and

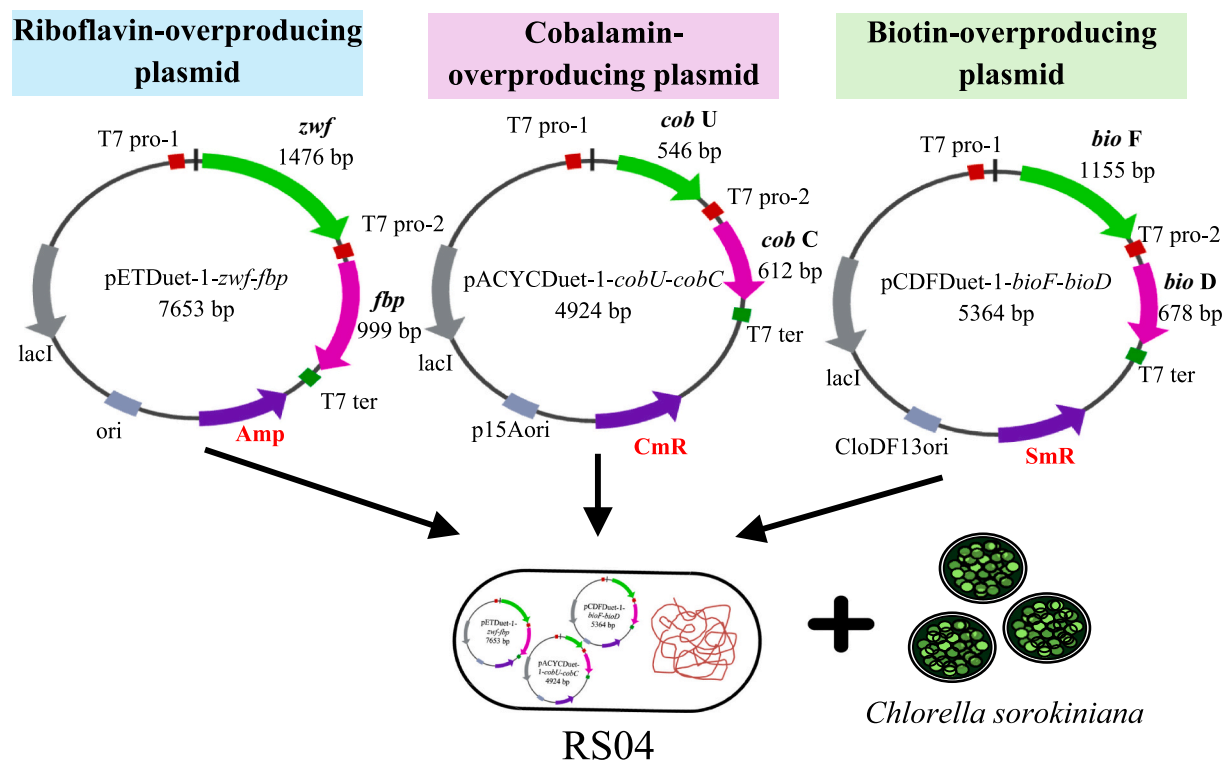


Fig. 1. Construction of recombinant *E. coli* RS04 harboring three separate plasmids, which are corresponding to riboflavin, cobalamin, and biotin synthesis, respectively. *Zwf*, glucose-6-phosphate 1-dehydrogenase; *fbp*, fructose-1,6-biphosphate I; *cobU*, bifunctional adenosylcobalamin biosynthesis protein; *cobC*, adenosylcobalamin/alpha-ribazole phosphatase; *BioF*, 7-keto-8-amino pelargonic acid synthase; *BioD*, desthiobiotin synthase; *Amp*, ampicillin resistance gene; *CmR*, chloramphenicol resistance gene; *SmR*, streptomycin resistance gene.

incubated under microalgal culture conditions for one week (for strain screening), and 28 days (for long-term culture stability assessment). During the long-term co-cultivation experiment, data were collected at seven-day intervals.

2.4. Quantification of targeted metabolites secreted into the extracellular medium

5 mL of sample was harvested at every data collection point for all the analysis. Gathered samples were centrifuged at 19,000 $\times g$ for 10 min and the supernatant was transferred into a clean sample tube. For the quantification of riboflavin, measurement was carried out with the supernatant at A_{444} immediately (Supplementary data S3), based on its intrinsic fluorescence that arises from its isoalloxazine ring structure [20]. To determine the concentration of cobalamin via a slightly modified method, 10 μ L of the aqueous supernatant was subjected to HPLC analysis using the Nexera Lite HPLC System (Shimadzu, Kyoto, Japan) equipped with a reversed-phase column (Cosmosil 5C18-AR-II, Φ 4.6 \times 250 mm, Nacalai Tesque, Kyoto, Japan) and a photodiode array detector set at A_{361} , exploiting the strong absorbance of its corrin structure. The HPLC system was implemented using solvent A (0.025 % trifluoroacetic acid in water, pH 2.6) and solvent B (acetonitrile), combined in a linear gradient. Elution was performed with solvent B from 0 %–70 % (0.21 min–10 min) at 30 °C, with a flow rate of 1 mL min^{-1} . A standard cyanocobalamin solution was prepared with the range of 0.625 to 10 mg L^{-1} [21]. Quantification of biotin was carried out using a bioassay method, employing *Lactiplantibacillus plantarum* NBRC 3070 (National Institute of Technology and Evaluation biological resource center, Kisarazu, Japan) as the indicator organism due to its absolute growth requirement for biotin. *L. plantarum* was cultured in 30 mL biotin-spiked Difco biotin assay medium (final concentration of 1 ng d-biotin mL^{-1}) for approximately 45 h at 37 °C to obtain an OD_{600} of approximately 2.0. The cells were centrifuged under aseptic conditions

and washed at least three times with sterile 0.9 % (w/v) NaCl solution and then re-suspended in 15 mL of biotin-free assay medium. Samples with various biotin concentrations were added and incubated under similar conditions for turbidimetric analysis at A_{600} . A standard curve was created for each assay [22].

2.5. Analytical methods

2.5.1. Determination of growth profile

Algal growth was assessed with the fluorescent intensity of Chl-a at excitation and emission wavelengths of A_{490} and A_{650} , respectively, using a microplate reader (SpectraMax M2, Molecular Devices, Sunnyvale, CA, USA). Chl-a would offer a practical indicator of algal population trends in mixed cultures as total optical density measurements cannot distinguish algal from bacterial biomass. Aliquots of harvested samples were serially diluted for the determination of bacterial colony-forming units.

2.5.2. Determination of photosynthetic pigment content

Remaining cell pellets from Section 2.4 were re-suspended with 3 mL of 2:1 chloroform: methanol (v/v) and allowed to stand at 4 °C overnight for chlorophyll extraction. Subsequently, 2 mL 0.9 % (w/v) NaCl solution was pipetted into the mixture to induce phase separation, resulting in two distinct layers: the lower chloroform phase was again transferred to a clean tube, whereas the upper aqueous phase was collected as intracellular organic materials (IOM) for further analysis in Section 2.5.3. Using the greenish lower phase, Chl-a/b, carotenoid, and total chlorophyll concentration were quantified based on all the key equations listed in previous work [23]. All the data were normalized by incorporating the relevant dilution factors.

2.5.3. Determination of biochemical composition

IOM was characterized for its total carbohydrate, protein, and lipid

content using phenol-sulfuric acid method [24], Bradford's Protein Assay (BIO-RAD Laboratories Inc. state, CA, according to the manufacturer's instructions), and the sulfo-phospho-vanillin method [25], respectively.

2.5.4. Determination of antioxidant enzyme activity

For catalase (CAT) activity determination, the reaction mixture was prepared with 10 mM phosphate buffer (pH 7.0), 30 mM H₂O₂, and cell lysate at a 25:5:2 ratio (v/v). The reaction was immediately started by adding H₂O₂ at 30 °C, and the decrease in the A₂₄₀ was measured. One unit of catalase activity (U) was defined as the amount of enzyme that decomposed 1 μmol H₂O₂ mg⁻¹ soluble protein per min [26]. Superoxide dismutase (SOD) activities were determined using SOD assay kit (Dojindo Laboratories, Kumamoto, Japan) according to the manufacturer's instructions. Peroxidase (POD) activities were determined based on the guaiacol oxidation method. Reaction mixture was prepared with 0.5 mL of cell lysate mixed with an equal volume of 50 mM phosphate buffer (pH 7) solution containing 20 mM guaiacol and 40 mM H₂O₂. A₄₇₀ was recorded every 1 min until a stable absorbance value was obtained. Similarly, one enzyme unit of POD was defined as the amount of enzyme that catalyzed the oxidation of 1 μmol of guaiacol per min and calculated using the molar extinction coefficient of guaiacol (26.6 mM⁻¹ cm⁻¹) [27].

2.5.5. Determination of fatty acid methyl esters (FAMEs)

The organic phase acquired in Section 2.5.2 was volatilized and methylated using a fatty acid methylation kit (Nacalai Tesque, Kyoto, Japan). Resulting supernatant was then analyzed using a gas chromatograph equipped with FID detector (Nexis GC-2030, Shimadzu Corporation, Kyoto, Japan) and TC-70 column (0.25 mm I.D. × 60 m, df = 0.25 μm). Chromatographic conditions were as follows: injection volume 1 μL; split ratio 1:50; air 300 mL min⁻¹; H₂ 35 mL min⁻¹; gas carrier (N₂) 30 mL min⁻¹; detector temperature 250 °C; oven temperature started at 140 °C for 3.5 min and raised to 180 °C at a rate of 8 °C min⁻¹, then ramped at 4 °C min⁻¹ to 200 °C, followed by a slower ramp of 1 °C min⁻¹ to 220 °C. The final ramping was 25 °C min⁻¹ to 240 °C and held for 3 min. The FAMEs contents were quantified by comparing their peak areas with that of 37-component FAME mix CRM47885 (Supelco, Bellefonte, PA, USA).

2.6. Evaluation of biofuel properties

To further assess the suitability of the fatty acid components from both mono- and co-cultures for biodiesel production, some pivotal properties of biodiesel derived from these fatty acids were evaluated. This evaluation involved theoretical calculations of various biodiesel properties as follows [28]:

$$\text{Average degree of unsaturation (ADU, %)} = \sum N \times M_f \quad (1)$$

where N is the number of carbon-carbon double bonds in each fatty acid, and M_f is the mass fraction of each fatty acid.

$$\text{Cetane number (CN)} = -6.6684 \times \text{ADU} + 62.876 \quad (2)$$

$$\text{Iodine value (IV, g I}_2 \text{100 g}^{-1} \text{oil)} = 74.373 \times \text{ADU} + 12.710 \quad (3)$$

$$\text{Kinematic viscosity (v}_i \text{, mm}^2 \text{s}^{-1}) = -0.613 \times \text{ADU} + 5.2065 \quad (4)$$

$$\text{Specific gravity } (\rho, \text{ g m}^{-3}) = 0.0055 \times \text{ADU} + 0.8276 \quad (5)$$

$$\text{Cloud point (CP, } ^\circ\text{C)} = -3.356 \times \text{ADU} + 19.994 \quad (6)$$

$$\text{Higher heating value (HHV, MJ kg}^{-1}) = 1.7601 \times \text{ADU} + 38.534 \quad (7)$$

$$\text{Long chain saturation factor (LCSF, wt\%)} = (0.1 \times C16$$

$$: 0) + (0.5 \times C18: 0) \quad (8)$$

$$\text{Cold filter plugging point (CFPP, } ^\circ\text{C)} = (3.1417 \times \text{LCSF}) - 16.477 \quad (9)$$

where C16:0 and C18:0 is the percentage of the saturated fatty acids.

$$\text{Oxidation stability (Y, h)} = \frac{117.9295}{X} + 2.5905 \quad (10)$$

where X is the content of linoleic and linolenic acids (wt%) (0 < X < 100).

2.7. Statistical analysis

Statistical analysis was conducted with SPSS Statistics 25 (SPSS Inc., Chicago, IL, USA). A one-way ANOVA and post-hoc Tukey-test were used to confirm the differences between experimental groups and controls, with significance indicated by a *p* < 0.05.

3. Results and discussion

3.1. Recombinant strains screening and long-term cultures growth assessment

A one-week-long co-culture system was preliminarily established to screen for the best recombinant strain with the best growth-enhancing effect (Fig. 2). According to Fig. 2, three recombinant strains, namely RS01, RS02, and RS03 each promoted at least a two-times increase in algal growth compared to the parental strain (PS) control. However, there were no significant differences in *C. sorokiniana* growth among these three recombinant strains (*p* > 0.5). As shown in Supplementary data S4, although riboflavin production in RS01 (7.8±0.4 mg L⁻¹) was approximately 10 times higher than that of PS (0.7±0.2 mg L⁻¹), its highest production did not give significant algal growth promotion effect when compared with RS02 and RS03, which exhibited lower riboflavin concentrations (4.3±3.0 mg L⁻¹ and 3.5±3.0 mg L⁻¹, respectively). Interestingly, a slight increase in cobalamin concentration in RS02 (0.10 ±0.00 mg L⁻¹, 1.1 % higher than PS) and biotin concentration in RS03 (0.38±0.04 ng mL⁻¹, 24 % higher than PS) resulted in a comparable growth-promoting effect for *C. sorokiniana*. This outcome allows the hypothesis that *C. sorokiniana* prioritizes certain vitamins for assimilation, a concept which will be discussed further in Section 3.2.

In the case of RS04, the synergistic effect of three vitamins further enhanced its cobalamin and biotin concentrations to 0.12±0.06 mg L⁻¹ and 0.39±0.08 ng mL⁻¹, respectively, but riboflavin production was decreased to 1.8±0.22 mg L⁻¹ (Supplementary data S4). Nevertheless, a striking color change of *Chl-a*, as seen in Fig. 2(a) for RS04, highlighted its most significant effect on boosting algal growth, resulting in a four-times increase in algal growth compared to PS (Fig. 2(b)). Given the simple cumulative effect, it was anticipated that RS04, harboring three plasmids responsible for the production of three essential vitamins, would result in approximately a six-times increase in algal growth, assuming a simple cumulative effect. However, the enhancing rate was diminished to a four-times. The reasons why simple additionality (synergistic effect) does not apply would be explained by several reasons: (a) the micronutrient utilization threshold has been reached in a resource-saturated state [29]; (b) the limitation of the current recombinant strategy-specifically the selection and expression of genes for vitamin overproduction in *E. coli* has not yet been fully optimized to achieve maximum metabolite yield that could benefit the existing co-culture system; (c) the vitamin uptake may have been inefficient due to a low abundance of suitable vitamin transport genes [12], resulting in limited vitamin availability for *C. sorokiniana*.

The results of RS04 were most favorable, making it the best candidate for the subsequent one-month-long experiment. This experiment

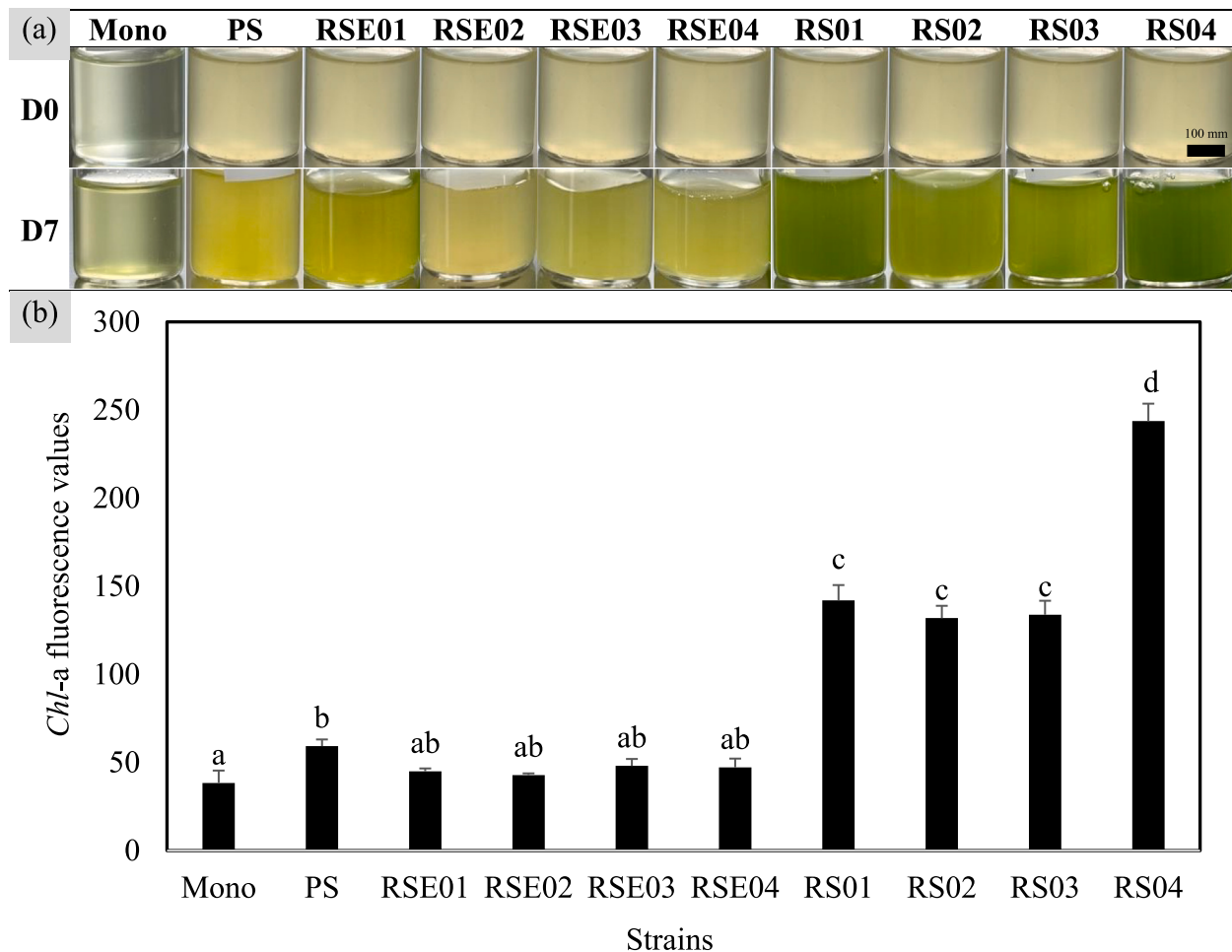


Fig. 2. Short-term one-week *C. sorokiniana*-*E. coli* co-cultures. (a) Images of cultures demonstrating the change in the culture color after seven days. (b) Chl-*a* fluorescence measurement after one-week-cultivation. Data are stated as mean±standard deviation, $n = 3$. Alphabets stand for significant differences between strains, detected by Tukey test. Mono: axenic microalgae; PS: parental strain; RSE01: *E. coli* BL21(DE3) with empty pETDuet-1; RSE02: *E. coli* BL21(DE3) with empty pACYCDuet-1; RSE03: *E. coli* BL21(DE3) with empty pCDFDuet-1; RSE04: *E. coli* BL21(DE3) with empty pETDuet-1, pACYCDuet-1, and pCDFDuet-1; RS01: *E. coli* BL21(DE3) with pETDuet-1-zwf-fbp; RS02: *E. coli* BL21(DE3) with pACYCDuet-1-cobU-cobC; RS03: *E. coli* BL21(DE3) with pCDFDuet-1-zwf-fbp; RS04: *E. coli* BL21(DE3) with pETDuet-1-zwf-fbp, pACYCDuet-1-cobU-cobC, and pCDFDuet-1-bioF-bioD. Detailed strain descriptions could be found in Supplementary data S1.

aimed to confirm that the findings obtained under short-term conditions were not temporary and to observe lipid accumulation under non-stressful conditions, making it more appropriate for application to large-scale. Fig. 3(a) shows a significant color change among the three studied groups, with results demonstrating that the algae grew the fastest with RS04 during the first 7 days, showing no obvious lag, implying its good adaptability to the cultivation environment. In Fig. 3(b), the growth of *C. sorokiniana* with PS displayed an S-shaped growth curve with the logarithmic growth period starting around D14, which was later than that of RS04. Both RS04 and PS had their maximal Chl-*a* fluorescence values of around 309 and 230 ($p < 0.05$), respectively, at D21, whereas monoculture (Mono) peaked earlier at D7 with a value of only 47. Generally, all three groups exhibited an exponential growth phase, followed by the onset of the stationary phase.

However, in Fig. 3(c), the bacterial densities in all groups drastically decreased in the first 7 days ($p < 0.05$), continued to decline until D14, and then slowly recovered thereafter. Such a growth recovery indicated that *C. sorokiniana* and PS or RS04 could grow in symbiosis in a medium containing organic carbon. Findings in this study were in agreement with Han et al. (2016) in which the bacterial concentration declined in the first 9 days, but steadily increased as the incubation time prolonged [30]. In the initial phase of the co-culture, exponentially growing algae tend to compete actively for more resources to dominate the entire system, thereby inhibiting bacterial growth. However, once algae

entered the stationary phase, algal by-products would have been released into the medium, allowing for a subsequent recovery of bacterial growth. For RS04, there could be an initial burden on the recipient bacterial metabolism but it recovered slowly once it adapted to the metabolic load. Another possible explanation lies in the efficiency of the phycosphere, where bacterial cells attach to the algal cell wall, ingest algal lysates (in close proximity) to support bacterial binary fission or plasmid replication, and finally release their offspring from the algal host cells to continue the cycle [31,32]. A well-maintained phycosphere could sustain the bacterial cells even when they are in low quantities or an inactive state.

Throughout the cultivation period, as displayed in Fig. 3(d), microalgae consistently dominated the co-culture system, maintaining a minimum microalgae-to-bacteria ratio of 1.2 and 6.2 in PS and RS04, respectively, from D7 onwards. The ratio in RS04 showed minimal fluctuations over time, attaining a peak of 8.1 at D21, whereas PS achieved a maximum ratio of 3.9 at D28 (during the algal stationary phase). It indicates a stable co-culture system without any issues of bacterial overgrowth. In short, overall trend throughout the entire experimental time course depicted that engineered bacterial strain produced slightly higher vitamin to support carbon assimilation, metabolism, and enhance redox reactions in microalgae. Additive effects of riboflavin by the engineered bacteria may lead to the formation of lumichrome as a degradation product, directly giving an early growth-boosting effect

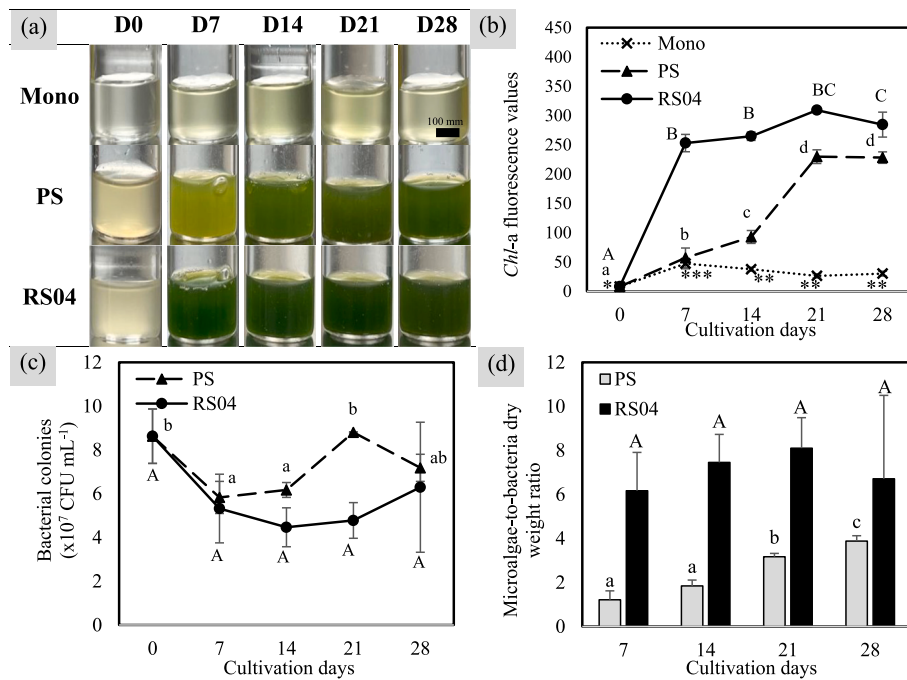


Fig. 3. Long-term 28-days *C. sorokiniana*-*E. coli* co-cultures. (a) Images of cultures demonstrating the change in the culture color over time. (b) *Chl-a* fluorescence measurement over time. (c) Colony-forming units (CFU) per mL from the co-cultures over time. (d) Microalgae-to-bacteria ratio (dry weight basis) over time. Data are stated as mean \pm standard deviation, $n = 3$. Alphabets stand for significant differences across different time points within the same strain, detected by Tukey test.

onto the microalgae [14,19]. Riboflavin is the precursor for flavin mononucleotide and flavin adenine dinucleotide, whereby these two are the cellular cofactor involved in biological redox and radical metabolism reactions to drive the ATP-dependent enzymatic reactions and stimulate

cell division [33]. While cobalamin being an enzymatic cofactor for methionine synthase activity, it is essential for the production of the universal methyl donor S-adenosylmethionine and for folate cycling necessary for DNA synthesis [34]. Last but not least, biotin serves as a

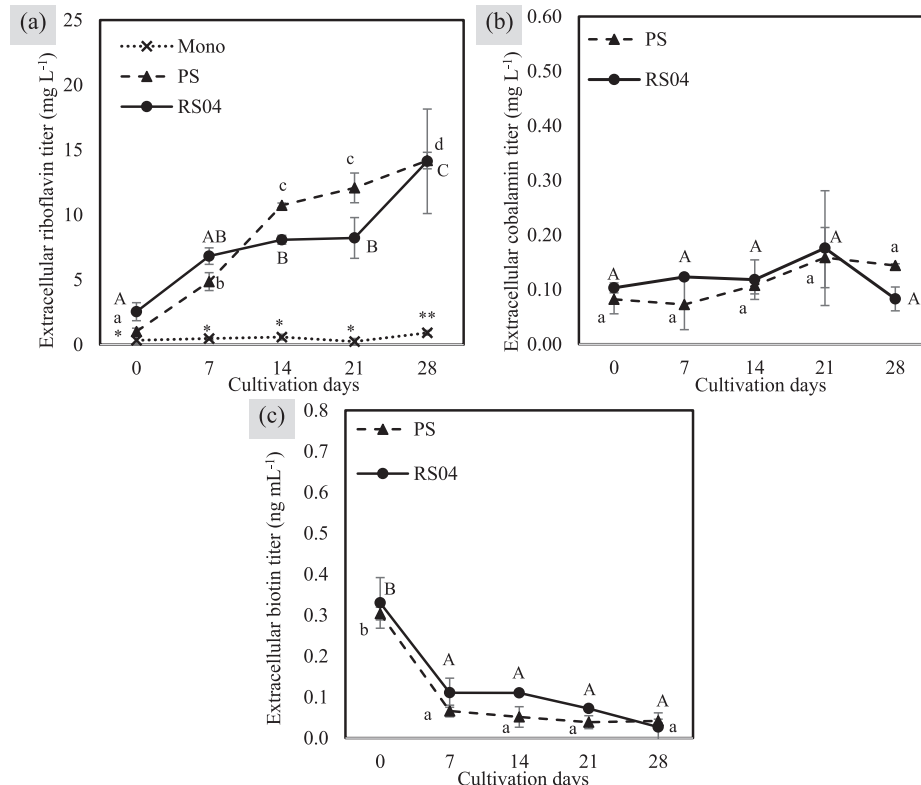


Fig. 4. Vitamin profiles of the extracellular medium across 28-days *C. sorokiniana*-*E. coli* co-cultures. (a) Riboflavin. (b) Cobalamin. (c) Biotin. Data are stated as mean \pm standard deviation, $n = 3$. Alphabets stand for significant differences across different time points within the same strain, detected by Tukey test.

cofactor for carboxylase enzymes such as acetyl-CoA carboxylase and pyruvate carboxylase which are preponderant for carbon fixation and gluconeogenesis, subsequently promoting both algal growth [29,35].

3.2. Vitamin profiles in extracellular medium throughout long-term cultivation

Representative profiles of riboflavin, cobalamin, and biotin assimilation were shown in Fig. 4. While *C. sorokiniana* could grow by scavenging vitamins from bacterial extracts, co-culture experiments demonstrated different assimilation trends across 28 days. With the presence of bacteria, riboflavin titer in the medium was at least three-times higher than that of Mono at D0 (Fig. 4(a)). The amount of riboflavin released into the medium remained consistent in Mono, whereas its production depicted an increasing trend for both PS and RS04 ($p < 0.05$). Notably, in RS04, the riboflavin concentration remained constant ($p > 0.5$) between D7 and D21 (6.8 mg L⁻¹ to 8.2 mg L⁻¹), but then increased further, eventually reaching the same level as PS (14.1±4.0 mg L⁻¹) by D28. The increasing microalgae-to-bacteria ratio from D7 to D21 indirectly indicated an active riboflavin assimilation by the cultures to support cell growth, as riboflavin plays a critical role as a cofactor in biological redox and radical metabolism [36]. Given that riboflavin production is generally bacterial cell density-driven, the attenuated rate of riboflavin uptake by the microalgae accounts for the observed accumulation from D21 onwards [14]. It simultaneously implied that riboflavin assimilation was governed by metabolic demand, with its utilization being selectively prioritized rather than constitutive.

On the other hand, in Fig. 4(b), there was no measurable cobalamin in *C. sorokiniana* cell extracts, confirming that the microalga does not synthesize cobalamin endogenously. Cobalamin is essential for the enzymatic activities of methionine synthase, class II ribonucleotide reductase (RNR II), and methylmalonyl-CoA-mutase (MMCM). In eukaryotic metabolism, microalgae generally require two different active forms of vitamin B₁₂: methylcobalamin (*MeCbl*) for catalysis in protein synthesis within the cytosol and adenosylcobalamin (*AdoCbl*) for enzymatic activity in the tricarboxylic acid cycle (TCA) within the mitochondrion [37]. Nonetheless, while *E. coli* lacks the methylation pathway necessary for *MeCbl* synthesis, the cobalamin detected predominantly exists in its native *AdoCbl* form. It then serves as a cofactor in the TCA cycle, powering cellular processes and effectively redirecting more carbon into microalgal biomass production. The minor fluctuations ($p > 0.05$) noted in Fig. 4(b) might reflect a consistent demand for cobalamin by the cultures throughout the co-cultivation period. Such a dynamic equilibrium was also evidenced by *Chlorella vulgaris*-anaerobic bacteria grown in tris acetate phosphate medium, where the uptake of cobalamin in the non-axenic culture system was attributed to the biosynthesis of symbiotic bacteria [38]. Previous research indicated that microalgae require only a minimum cobalamin of 10 ng L⁻¹ for growth, whereas ~0.1 mg L⁻¹ achieved in the medium appeared to be more than sufficient [10,39,40]. As cobalt serves as a critical precursor for cobalamin synthesis and only becomes limiting at <0.01 mM, 0.17 mM cobalt nitrate hexahydrate from BG11 medium (~10 mg L⁻¹ cobalt ions) effectively supported high production noted in this study, which aligns with expectations. As a result, this level was likely adequate to maintain a balance between bacterial production and algal uptake. Nevertheless, although cobalamin levels remained consistent throughout the co-cultivation period, this observation may reflect the presence of residual cobalamin produced by the bacteria prior to co-cultivation, rather than continuous synthesis during the interaction. Hence, the proposed role of cobalamin is currently presented as a potential hypothesis based on the available data.

Interestingly, in Fig. 4(c), biotin concentration was significantly decreasing ($p < 0.05$) during the first seven days, as it is another important coenzyme for carboxylation reactions and fatty acid synthesis during algae's rapid proliferation phase [35]. Since *C. sorokiniana* does not produce biotin de novo, an initial burst in algal growth likely

involved the scavenging of substantial biotin amounts from external sources to support cell division and this early amount decrement could also be associated to nutrient storage for subsequent growth. As the culture progresses, the decrement may stabilize, as indicated in Fig. 4(c). However, a previous research showed that 1 ng mL⁻¹ biotin was optimal for green microalgal growth, while the current study found only a maximum of 0.3 ng mL⁻¹ biotin, still below the algae's full uptake capacity [29]. This directly explained the continuous decrease of biotin after D7. Aside from that, Suneerat and others (2018) also discovered that a 50: 0.5: 1 ng mL⁻¹ mixture of thiamine: biotin: cobalamin managed to achieve 1.86 g L⁻¹ algal biomass, highlighting the equivalent importance of both biotin and cobalamin for algal growth, which was in line with the current findings. Another possible explanation could be bacterial self-consumption or reduced synthesis of bacterial biotin under interactive conditions, rather than exclusive uptake by the microalga alone. As the current dataset in this work does not permit clear discrimination among these possibilities, explanation is provided as a working hypothesis derived from observed results.

In short, the entire co-culture system revealed possible distinct temporal patterns in the vitamin assimilation, shaped by the metabolic demands of the algae and vitamin availability in the medium. Biotin was rapidly taken up during the early growth phase, cobalamin maintained a steady profile throughout cultivation. In contrast, riboflavin decline-ment was more gradual and closely tied to bacterial production and algal density. Therefore, the overall synergistic interactions between three different vitamins allow a proposal of sequential vitamin assimilation model as follows: biotin (initial uptake) → cobalamin (consistent need) → riboflavin (slowest).

3.3. Effect of engineered bacterial strain onto photosynthetic pigment and intracellular organic matters composition

Microalgae produce and accumulate different compounds depending on the cultivation environment that are applied during their growth. For instance, Chl-a-to-b ratio reflects the adaptation of the light-harvesting complex whereas carotenoid content provides information on the photoprotective mechanisms which safeguard photosystems against oxidative stress [41,42]. These indicators illustrate how microalgal cells adjusted their photosynthetic apparatus and photoprotective capacity in response to the co-cultivation conditions. As shown in Fig. 5(a) and (b), two main groups of pigments: Chl-a,b (most abundant in green microalgae) and carotenoids- were quantified in cultivated *C. sorokiniana* under the effect of RS04. Chl-a is a principal photosynthetic pigment to capture light energy whereas Chl-b acts as an accessory pigment that responsible for energy transfer to Chl-a for light harvesting efficiency enhancement [43]. In Fig. 5(a), low Chl-a-to-b ratio (~0.45 to ~0.55) found in RS04 across the entire cultivation timeframe indicates that the co-cultures were subjected to low light intensities or shaded conditions due to high-dense cultures as noted in RS04 from D7 onwards. In parallel with the findings of this study, Chl-a content in *Tetraselmis suecica* was reduced because of lower light penetration within the culture [44]. Expectedly, the Chl a/b ratio increased to support more photosynthesis in less dense Mono, whereas exponentially growing PS depicted a decline in the ratio after D7.

Since there was no excess light energy to dissipate RS04 groups (due to shaded conditions), no photoprotection from carotenoids is needed. As a result, in Fig. 5(b), the carotenoid content remained significantly low (4.2 % to 5.45 %) from D7 onward [45]. As expected, carotenoid production was highest in Mono, followed by PS. In Fig. 5(c), the similarity between the total pigment production and the growth profile mirrors a direct correlation between the two. Additional vitamin supplementation from RS04 rendered a 3.5-times higher total pigment production than PS at D7, confirming their roles in promoting the biological activity of algal cells. It has also been evidenced by a *Chlorella vulgaris*-*Bacillus licheniformis* co-culture system grown in synthetic wastewater with exogenous vitamin B, where differential protein

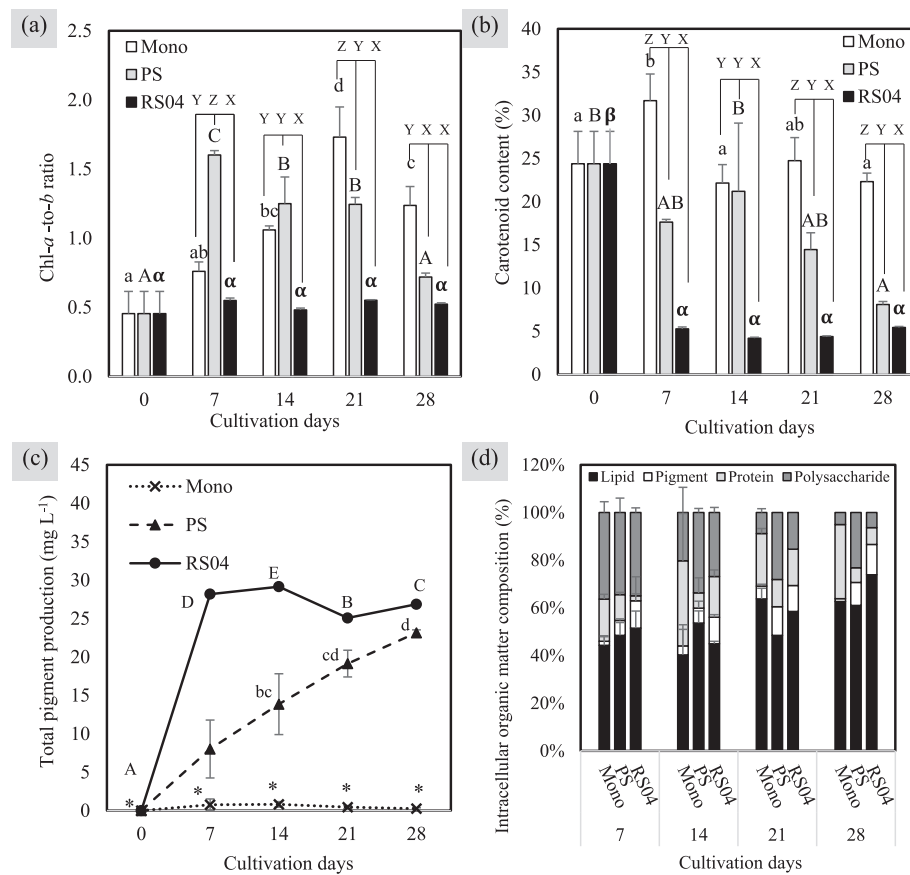


Fig. 5. Photosynthetic pigments in *C. sorokiniana*-*E. coli* co-cultures over 28-days of co-cultivation. (a) Ratio of chlorophyll *a* to chlorophyll *b*. (b) Carotenoid content. (c) Total chlorophyll production. (d) Intracellular metabolites profile in the co-culture system. Data are stated as mean \pm standard deviation, $n = 3$. Lowercase alphabets, uppercase alphabets, and Greek letters stand for significant differences across different time points within the same strain, detected by Tukey test. XYZ show significant differences among control and different strains at same time points (one-way ANOVA; Tukey multiple comparison; $p < 0.05$).

enrichment in GO terms was significant for chloroplast, lipid synthesis, intracellular protein metabolism, material transports, and transmembrane transport [13].

Intracellular biochemical composition from the cultures was also summarized in Fig. 5(d). Lipids typically constitute the largest proportion within the algal cells, followed by carbohydrates, proteins, and pigments, with its total lipid content accounting for up to $73.9 \pm 4.43\%$ of the intracellular organic matter. Essentially, enhanced lipid accumulation observed in co-cultures could be attributed to the increased biomass productivity, highlighting the role of elevated glucose-6-phosphate dehydrogenase (G6PDH) enzymatic activities in supplying additional NADPH for fatty acid biosynthesis [46]. Notably, the carbohydrate content gradually decreased over time, accompanied by a slow rise in lipid content. Results are consistent with a previous study reporting that during reduced CO_2 fixation, *Chlamydomonas* sp. KOR1 exhibited rapid carbohydrate degradation alongside increased lipid accumulation [47]. Carbohydrates typically serve as short-term energy reserves due to their faster synthesis and metabolism during the active cell division phase. However, under nutrient-depleted conditions, central carbon metabolism shifts toward lipid accumulation for long-term energy storage [48]. It is also coupled with the onset of oxidative stress, a phenomenon that will be detailed in the subsequent Section 3.4.

3.4. Effect of engineered bacterial strain onto the oxidative stress responses in the cultures

Microalgae generate reactive oxygen species (ROS) such as O_2^- and H_2O_2 under stress while antioxidants could effectively scavenge these ROS to safeguard the microalgal cellular components from oxidative

damage [49]. As depicted schematically in Fig. 6, at D7, the activities of CAT, SOD, and POD were relatively lower in PS but comparably higher in RS04, as compared to Mono. It is common to report lower antioxidant enzyme activities in co-cultures compared to monocultures of the same species as less O_2^- and H_2O_2 were produced in co-cultures. This is due to their ability to balance intracellular antioxidant systems to mitigate oxidative stress while achieving the desired biomass yield, preventing lipid oxidation and enhancing lipid productivity [28].

However, an exceptionally high antioxidant activity observed in RS04 at D7 and a significant drop afterwards in this study might warrant careful attention. While metabolic activity in algal cultures with RS04 was likely at its peak at D7, an oxidative burst was stemming from biotic stress, such as heightened mitochondrial electron transport chain (in microalgae) and oxidative phosphorylation (in bacteria) [50]. Excess oxygen accumulation during active photosynthesis in microalgae could have generated more ROS, eventually exceeding the ROS scavenging capacity of auto-oxidizing enzymes (superoxide dismutase, ascorbate peroxidase, catalase, glutathione peroxidase, etc.) present in the chloroplast. The same effect could also be seen when the algal population has attained its peak in the case of PS. Nevertheless, the ROS produced did not appear to overwhelm the microalgal protective mechanisms, as no severe growth reduction was observed afterwards. Instead, a rapid decline following that suggested a cellular self-adjustment to maintain physiological homeostasis [26]. This scenario could also be managed as a stress-priming effect during the optimal growth stages, enabling the cells to handle ROS more efficiently throughout the subsequent growth phase.

Evidently, antioxidation activities in RS04 were comparatively lower than both Mono and PS from D14 onwards. A gradual rise of those

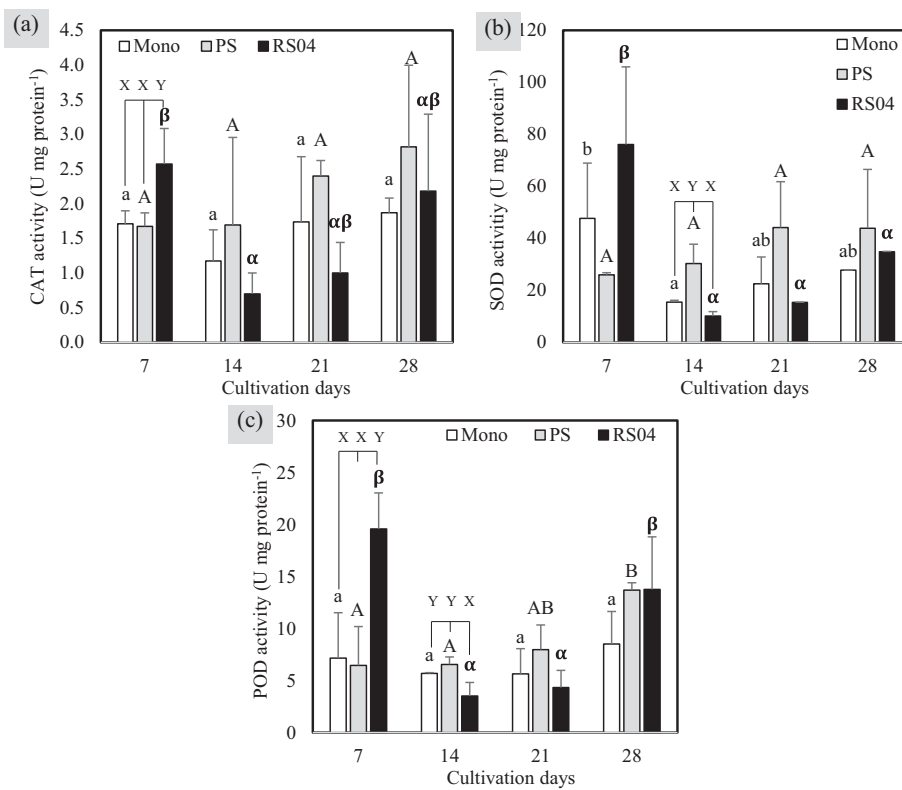


Fig. 6. Antioxidant enzyme activities of *C. sorokiniana*-*E. coli* co-cultures over 28-days of co-cultivation. (a) Catalase. (b) Superoxide dismutase. (c) Peroxidase. Data are stated as mean±standard deviation, $n = 3$. Lowercase alphabets, uppercase alphabets, and Greek letters stand for significant differences across different time points within the same strain, detected by Tukey test. XYZ show significant differences among control and different strains at same time points (one-way ANOVA; Tukey multiple comparison; $p < 0.05$).

activities for all the studied sample groups was attributed to the abiotic stress, such as nutrient limitation, as seen in many former studies [51,52]. Cells experiencing interspecies competition or nutritional stress would typically activate the synthesis of reserve compounds like lipids, as part of their survival strategy. Upregulating diacylglycerol acyltransferase (DGAT) and inhibiting ADP-glucose pyrophosphorylase were some key regulatory mechanisms that are activated under environmental stress [53]. The overall antioxidant activities have indirectly validated the lipid accumulation trend observed in the biochemical indices.

3.5. FAME contents and fatty acids-based biodiesel properties evaluation

The fatty acid profile of algae determines its potential as a biodiesel feedstock. As tabulated in Table 1, the biomass lipids obtained from the pure algal culture (Mono condition) consisted mainly of C16:0, C18:0, and C18:2. At least 80 % of the fatty acids were saturated. Notably, a percentage increase of the only PUFA (C18:2) in Mono from D7 (4.5 ± 1.4 %) to D14 (13.7 ± 7.8 %) could indicate the adaptive stress response in the cultures from D14 onwards. As the culture ages, cultures introduced a lipid remodeling by increasing their PUFA content in the membrane lipids to maintain the cellular membrane fluidity and functionality [54,55]. While being non-polar lipids, triacylglycerols, which contain C16:0 and C18:0, serve as energy storage molecules. Their gradual decline over time confirmed a trend of lipid remodeling [54]. A similar profile was also observed in both PS and RS04 across the cultivation time.

However, when comparing to that of Mono group, co-cultures offered a great variety of fatty acids, namely C12:0, C13:0, C14:0, C15:0, C15:1, C16:1, C17:0, C17:1, C18:1, and C18:3. All these fatty acids primarily originated from the symbiotic bacterium *E. coli*, as supported by a previous findings [56]. Although a higher fatty acid

contribution was anticipated from the microalgae in co-cultures with a high microalgae-to-bacteria ratio, the lower-than-expected findings (up to 57 %) were likely due to the incorporation of bacteria-derived fatty acids into the microalgae's lipid pool from the exogenous medium [57,58]. Despite that, both the PS and RS04 were able to accumulate a significant amount of MUFA but exhibited a contrasting trend between the two over time, most likely due to their huge difference in algal specific growth rate. While high MUFA content is beneficial for biodiesel production [59], PS required 21 days to reach its maximum MUFA content (12.0 ± 1.4 %), whereas RS04 attained the same level in just 7 days (11.10 ± 0.2 %). The quicker attainment of the same MUFA level suggests enhanced lipid metabolism and physiological maturation of algal cells under the influence of bacterial vitamin secretion from RS04. Higher induced ATP and NADPH production from these vitamins at early co-cultivation phase (D7) are essential in fatty acid biosynthesis flux, allowing earlier buildup of lipid intermediates, like MUFA. Aside from that, functioning as an essential cofactor for carboxylase enzymes, higher exogenous biotin level availability (as detected in RS04 co-culture extracellular medium- Fig. 4(c)) caused a decrease of C18:1 and an increase of C18:2 in RS04 co-culture, as compared to PS group. Similar observation was in parallel with a former study citing that such an opposite trend of C18:1 and C18:2 was probably contributed to a biotin-regulated fatty acid desaturase [60]. Also, a combination of C16-C18 fatty acids accounted for a maximum of 67 % and 64 % for PS and RS04, respectively, which were comparatively higher than that of Mono (61 %).

To better align with the desired biodiesel standards, Table 2 presents an assessment of the estimated properties of fatty acids-based biodiesel. The theoretical values of all biodiesel parameters fully met the criteria set by both ASTM D6751 and EN 14214 standards. Cetane number (CN) is a major indicator of biodiesel quality associated with combustion quality and ignition delay time, with a higher value signifying a better

Table 1

Fatty acid profiles in monocultures and co-cultures over time.

Fatty acid profiles	Mono				PS				RS04			
	D7	D14	D21	D28	D7	D14	D21	D28	D7	D14	D21	D28
Lauric acid (C12:0)	–	–	–	–	1.1±0.1	0.6±0.2	0.4±0.0	0.3±0.1	0.7±0.1	0.7±0.1	0.5±0.1	0.5±0.1
Tridecanoic acid (C13:0)	–	–	–	–	0.6±0.1	2.6±0.3	1.9±0.3	2.8±0.0	4.0±0.1	4.8±0.1	4.7±0.1	4.8±0.2
Myristic acid (C14:0)	–	–	–	–	1.9±0.1	1.3±0.2	1.0±0.0	1.2±0.0	0.9±0.0	0.8±0.1	0.9±0.0	0.9±0.1
Pentadecanoic acid (C15:0)	–	–	–	–	1.0±0.1	0.8±0.1	0.7±0.1	0.8±0.1	1.1±0.1	0.8±0.1	0.7±0.1	0.7±0.1
cis-10-pentadecenoic acid (C15:1)	–	–	–	–	1.4±0.1	1.6±0.8	2.1±0.3	3.0±0.1	5.1±0.3	6.4±0.2	6.0±0.1	5.6±0.4
Palmitic acid (C16:0)	52.0±0.9	43.5±3.2	42.0±2.9	44.3±3.4	35.6±0.9	30.9±2.1	27.3±0.9	26.8±0.4	28.9±0.8	23.3±0.3	24.8±0.5	24.5±0.4
Palmitoleic acid (C16:1)	–	–	–	–	1.3±0.1	2.4±0.1	3.9±0.7	4.7±0.4	5.5±0.2	5.8±0.1	5.2±0.2	5.2±0.1
Heptadecanoic acid (C17:0)	–	–	–	–	2.1±0.6	3.9±1.3	4.7±0.2	4.6±0.1	7.1±0.3	9.0±0.3	9.2±0.2	9.2±0.2
Heptadecenoic acid (C17:1)	–	–	–	–	20.7±0.9	17.3±0.8	14.9±1.0	14.8±0.6	6.9±0.1	7.0±0.2	7.1±0.1	8.0±0.4
Stearic acid (C18:0)	43.5±0.7	42.8±5.4	38.6±5.9	44.5±2.3	15.6±1.4	12.5±2.2	7.5±0.3	7.5±0.5	13.4±0.8	8.5±0.1	8.2±0.3	6.8±0.7
Oleic acid (C18:1)	–	–	–	–	4.9±0.2	5.3±1.4	8.2±0.8	6.9±0.3	5.5±0.0	5.4±0.1	3.5±0.2	3.0±0.1
Linoleic acid (C18:2)	4.5±1.4	13.7±7.8	19.5±3.4	11.2±5.7	5.2±1.7	12.2±2.0	19.1±1.2	18.2±0.9	14.3±0.7	20.4±0.4	21.5±0.2	21.7±0.7
Linolenic acid (C18:3)	–	–	–	–	8.5±0.5	8.6±0.6	8.4±0.2	8.5±0.1	6.6±0.1	7.2±0.4	7.7±0.4	9.1±0.6
Σ C16	52.0±0.9	43.5±3.2	42.0±2.9	44.3±3.4	36.9±1.0	33.3±2.0	31.1±1.6	31.5±0.4	34.4±0.6	29.1±0.3	30.0±0.4	29.7±0.5
Σ C18	4.5±1.4	13.7±7.8	19.5±3.4	11.2±5.7	18.7±1.9	26.0±3.5	35.7±0.3	33.6±1.1	26.4±0.7	32.9±0.1	32.6±0.3	33.8±1.0
Σ C16 + C18	56.5±0.7	57.2±5.4	61.4±5.9	55.5±2.3	55.5±0.9	59.4±1.8	66.8±1.3	65.1±0.8	60.8±0.1	62.0±0.3	62.6±0.5	63.5±0.6
Σ SFA	95.5±1.4	86.3±7.8	80.5±3.4	88.8±5.7	54.1±2.2	45.3±4.3	36.2±0.6	35.8±0.8	43.9±1.6	33.3±0.3	34.5±0.7	32.7±1.2
Σ MUFA	–	–	–	–	6.2±0.3	7.7±1.6	12.0±1.4	11.5±0.5	11.1±0.2	11.2±0.1	8.6±0.4	8.2±0.1
Σ PUFA	4.5±1.4	13.7±7.8	19.5±3.4	11.2±5.7	13.7±2.1	20.8±2.1	27.5±1.1	26.8±0.9	20.8±0.7	27.6±0.1	29.2±0.3	30.8±1.1
Others	–	–	–	–	25.9±0.7	26.2±2.3	24.2±1.1	25.9±0.5	24.3±0.7	27.9±0.2	27.7±0.4	28.3±0.2

SFA, MUFA, and PUFA indicate saturated fatty acids, monounsaturated fatty acids, and polyunsaturated fatty acids, respectively. Other represented the components other than C12, C14, C16, and C18. The data are shown as the mean value of three independent biological replicates ($n = 3$) \pm the standard deviation.

Table 2

The estimated properties of monoculture and co-cultures fatty acids-based biodiesel in comparison with the international standards over time.

Biodiesel parameters	Units	Mono				PS				RS04				International standards	
		D7	D14	D21	D28	D7	D14	D21	D28	D7	D14	D21	D28	ASTM D6751	EN 14214
Cetane number (CN)	N/A	62.3	61.1	60.3	61.4	60.1	59.0	57.8	58.0	58.9	58.0	57.9	57.6	≥ 47	≥ 51
Iodine value (IV)	g I ₂ 100 g oil ⁻¹	19.4	33.0	41.7	29.4	44.1	55.7	68.9	67.4	56.8	67.3	68.2	71.4	N/A	≤ 120
Average degree of unsaturation (ADU)	N/A	0.1	0.3	0.4	0.2	0.4	0.6	0.8	0.7	0.6	0.7	0.7	0.8	N/A	N/A
Oxidation stability (Y)	h	28.9	11.2	8.7	13.1	11.2	8.3	6.9	7.0	8.3	6.9	6.6	6.4	N/A	≥ 6
Kinematic viscosity (ν_i)	mm ² s ⁻¹	5.2	5.0	5.0	5.1	4.9	4.9	4.7	4.8	4.8	4.8	4.7	4.7	1.9–6.0	3.5–5.0
Specific gravity (ρ)	g m ⁻³	0.9	0.9	0.9	0.9	0.9	0.9	0.9	0.9	0.9	0.9	0.9	0.9	0.878	0.86–0.90
Cloud point (CP)	°C	19.7	19.1	18.7	19.2	18.6	18.1	17.5	17.5	18.0	17.5	17.5	17.3	N/A	>4
Long chain saturation factor (LCSF)	wt%	0.3	0.3	0.2	0.3	0.1	0.1	0.1	0.1	0.1	0.1	0.1	0.1	N/A	N/A
Cold filter plugging point (CFPP)	°C	-15.6	-15.7	-15.7	-15.6	-16.1	-16.2	-16.3	-16.3	-16.2	-16.3	-16.3	-16.3	N/A	≤ 5 or ≥ -20
Higher heating value (HHV)	MJ kg ⁻¹	38.7	39.0	39.2	38.9	39.3	39.6	39.9	39.8	39.6	39.8	39.9	N/A	N/A	N/A

engine performance. In this study, all the groups have shown a similar CN of ~60. Iodine value (IV), a rough measure of oxidative stability, with high IV indicating lower stability, unfortunately, shows that both PS and RS04 have poorer oxidative stability. The same applies to the

average degree of unsaturation (ADU) and oxidation stability (Y), which reflects the oxidative stability of biodiesel during long-term storage. A higher ADU value in both PS and RS04 was significantly associated with their high PUFA content [29].

A qualified biodiesel should have low kinematic viscosity (ν_i), as depicted by both PS and RS04. Simultaneously, a specific gravity (ρ) of 0.9 g m^{-3} reflects effortless transportability of these fatty acids-based biodiesel. Cloud point (CP), is the lowest temperature at which biodiesel starts to form crystals. An average value of $\sim 18^\circ \text{C}$, across all the groups and time, suggests an improved biodiesel applicability under colder climates. Associating with this, the long chain saturation factor (LCSF) and the cold filter plugging point (CFPP), are another biodiesel parameters to indicate the flow performance at low temperature, with a lower value predicting a better flow performance. All the co-cultures demonstrated a lower value, showing that symbiotic bacteria could improve this specific biodiesel property. A high HHV value derived from all the groups represents a higher power output delivery per unit of fuel, and the average value ($\sim 40 \text{ MJ kg}^{-1}$) acquired in this study was in line with the previous recommendation [28,61].

Although *C. sorokiniana* co-cultured with RS04 did not show significant improvements in biodiesel properties compared to the controls, all theoretical values still met international criteria and remained competitive with fossil fuels. Remarkably, RS04 group exhibited an exceptionally high algal growth rate and required minimal cultivation time to achieve high biomass and lipid productivity. The synergistic effects of the vitamin-producing bacteria primarily enhanced lipid yield without compromising cell viability, reflecting a high cultivation system stability in long-term.

4. Conclusion

RS04 harboring riboflavin, cobalamin, and biotin-related genes was found to remarkably enhance the *C. sorokiniana* growth by at least five times just within seven days, when compared to both Mono and PS control groups. The synergistic effects were encouraging when a alga-*RS04* co-culture managed to give an extremely high microalgal-to-bacterial ratio of 6.2, which was five-times higher than the PS group. The findings also suggest that co-cultures exhibited a prioritized vitamin assimilation pattern, with biotin being taken up early, followed by a sustained demand of cobalamin, while riboflavin was only required when needed at a later phase. From D14 onwards, all the culture groups appeared to experience environmental stress, as reflected by a rising trend in total lipid after a potential metabolic shift. Co-cultures yielded a huge variety of fatty acids, with C16-C18 more than 56 %. However, further efforts are still necessary as RS04 did not significantly impact the biodiesel properties, although its extraordinarily high biomass and lipid productivity could potentially offset the limitation.

CRediT authorship contribution statement

C.Y. Tong: Writing – review & editing, Writing – original draft, Validation, Methodology, Investigation, Formal analysis, Data curation, Conceptualization. **Hiroya Tomita:** Writing – review & editing, Supervision, Resources, Methodology. **Kentaro Miyazaki:** Writing – review & editing, Resources. **C.J.C. Derek:** Writing – review & editing, Supervision. **Kohsuke Honda:** Writing – review & editing, Supervision, Funding acquisition.

Declaration of competing interest

The authors declare that they have no known competing financial interests or personal relationships that could have appeared to influence the work reported in this paper.

Acknowledgement

This work was partly supported by GteX Program Japan Grant Number JPMJGX23B4.

Appendix A. Supplementary data

Supplementary data to this article can be found online at <https://doi.org/10.1016/j.algal.2025.104442>.

Data availability

The datasets generated during and/or analyzed during the current study are available from the corresponding author on reasonable request.

References

- [1] A. Ray, M. Nayak, A. Ghosh, A review on co-culturing of microalgae: a greener strategy towards sustainable biofuels production, *Sci. Total Environ.* 802 (2022) 149765.
- [2] M. Wang, X. Ye, H. Bi, Z. Shen, Microalgae biofuels: illuminating the path to a sustainable future amidst challenges and opportunities, *Biotechnol. Biofuels Bioprod.* 17 (2024) 10.
- [3] H. Jin, H. Zhang, Z. Zhou, K. Li, G. Hou, Q. Xu, W. Chuai, C. Zhang, D. Han, Q. Hu, Ultrahigh-cell-density heterotrophic cultivation of the unicellular green microalga *Scenedesmus acuminatus* and application of the cells to photoautotrophic culture enhance biomass and lipid production, *Biotechnol. Bioeng.* 117 (2020) 96–108.
- [4] S. Kim, M. Moon, M. Kwak, B. Lee, Y.K. Chang, Statistical optimization of light intensity and CO_2 concentration for lipid production derived from attached cultivation of green microalga *Ettlia* sp, *Sci. Rep.* 8 (2018) 15390.
- [5] M.S. Rana, S.K. Prajapati, Stimulating effects of glycerol on the growth, phycoremediation and biofuel potential of *Chlorella pyrenoidosa* cultivated in wastewater, *Environ. Technol. Innovation* 24 (2021) 102082.
- [6] B. Zhang, W. Li, Y. Guo, Z. Zhang, W. Shi, F. Cui, P.N.L. Lens, J.H. Tay, Microalgal-bacterial consortia: from interspecies interactions to biotechnological applications, *Renew. Sust. Energ. Rev.* 118 (2020) 109563.
- [7] D.E. Berthold, K.G. Shetty, K. Jayachandran, H.D. Laughinghouse, M. Gantar, Enhancing algal biomass and lipid production through bacterial co-culture, *Biomass Bioenergy* 122 (2019) 280–289.
- [8] X. Zhou, W. Jin, Q. Wang, S. Guo, R. Tu, S.-F. Han, C. Chen, G. Xie, F. Qu, Q. Wang, Enhancement of productivity of *Chlorella pyrenoidosa* lipids for biodiesel using co-culture with ammonia-oxidizing bacteria in municipal wastewater, *Renew. Energy* 151 (2020) 598–603.
- [9] Y. Chu, X. Jiao, D. Li, J. Yu, C. Wang, M. He, Integration of dairy manure wastewater treatment and biofuel production by microalgae-bacteria consortia in a biofilm reactor, *Algal Res.* 86 (2025) 103912.
- [10] P. Tandon, Q. Jin, L. Huang, A promising approach to enhance microalgae productivity by exogenous supply of vitamins, *Microb. Cell Factories* 16 (2017) 219.
- [11] M.A.A. Grant, E. Kazamia, P. Cicuta, A.G. Smith, Direct exchange of vitamin B12 is demonstrated by modelling the growth dynamics of algal-bacterial cocultures, *ISME J.* 8 (2014) 1418–1427.
- [12] C.K. Madhubalaji, S. Ravi, S.N. Mudliar, Unraveling of *Chlorella*-associated bacterial load, diversity, and their imputed functions at high- and low-yield conditions through metagenome sequencing, *J. Phycol.* 58 (2022) 133–145.
- [13] X. Ji, X. Luo, J. Zhang, D. Huang, Effects of exogenous vitamin B12 on nutrient removal and protein expression of algal-bacterial consortium, *Environ. Sci. Pollut. Res.* 28 (2021) 15954–15965.
- [14] B.R. Lopez, O.A. Palacios, Y. Bashan, F.E. Hernández-Sandoval, L.E. de Bashan, Riboflavin and lumichrome exuded by the bacterium *Azospirillum brasiliense* promote growth and changes in metabolites in *Chlorella sorokiniana* under autotrophic conditions, *Algal Res.* 44 (2019) 101696.
- [15] N. Hakalin, A. Paz, D. Gomes Aranda, L. Moraes, Enhancement of cell growth and lipid content of a freshwater microalga *Scenedesmus* sp. by optimizing nitrogen, phosphorus and vitamin concentrations for biodiesel production, *Nat. Sci.* 06 (2014) 1044–1054.
- [16] A. Fazeli Danesh, P. Mooij, S. Ebrahimi, R. Kleerebezem, M. van Loosdrecht, Effective role of medium supplementation in microalgal lipid accumulation, *Biotechnol. Bioeng.* 115 (2018) 1152–1160.
- [17] A.K. Sharma, P.K. Sahoo, S. Singhal, A. Patel, Impact of various media and organic carbon sources on biofuel production potential from *Chlorella* spp, 3, *Biotech* 6 (2016) 116.
- [18] C.Y. Tong, H. Tomita, K. Miyazaki, C.J.C. Derek, K. Honda, KEIO knockout collection reveals metabolic crosstalk in *Chlorella* spp-*Escherichia coli* co-cultures, *J. Phycol.* 61 (2025) 443–462.
- [19] C.Y. Tong, H. Tomita, K. Miyazaki, C.J.C. Derek, K. Honda, Impacts of riboflavin-overproducing engineered *Escherichia coli* towards *Chlorella sorokiniana* growth in co-cultivation approach, *Algal Res.* 86 (2025) 103938.
- [20] Z. Lin, Z. Xu, Y. Li, Z. Wang, T. Chen, X. Zhao, Metabolic engineering of *Escherichia coli* for the production of riboflavin, *Microb. Cell Factories* 13 (2014) 104.
- [21] H. Fang, D. Li, J. Kang, P. Jiang, J. Sun, D. Zhang, Metabolic engineering of *Escherichia coli* for de novo biosynthesis of vitamin B12, *Nat. Commun.* 9 (2018) 4917.
- [22] J. Mao, H. Fang, G. Du, D. Zhang, Enhancing biotin production in *Bacillus subtilis*: overcoming native pathway limitations, *Process Biochem.* 145 (2024) 122–130.

[23] S. Chai, J. Shi, T. Huang, Y. Guo, J. Wei, M. Guo, L. Li, S. Dou, L. Liu, G. Liu, Characterization of *Chlorella sorokiniana* growth properties in monosaccharide-supplemented batch culture, *PLoS One* 13 (2018) e0199873.

[24] M. Dubois, K.A. Gilles, J.K. Hamilton, P.A. Rebers, F. Smith, Calorimetric method for determination of sugars and related substances, *Anal. Chem.* 28 (1956) 350–356.

[25] J. Park, H.J. Jeong, E.Y. Yoon, S.J. Moon, Easy and rapid quantification of lipid contents of marine dinoflagellates using the sulfo-phospho-vanillin method, *Algae* 31 (2016) 391–401.

[26] S. Sudarshan, V.S. Bharti, S. Harikrishnan, S.P. Shukla, G. RathiBhuvaneswari, Eco-toxicological effect of a commercial dye rhodamine B on freshwater microalgae *Chlorella vulgaris*, *Arch. Microbiol.* 204 (2022) 658.

[27] M. Drira, J. Ben Mohamed, H. Ben Hlima, F. Hentati, P. Michaud, S. Abdelkafi, I. Fendri, Improvement of *Arabidopsis thaliana* salt tolerance using a polysaccharidic extract from the brown algae *Padina pavonica*, *Algal Res.* 56 (2021) 102324.

[28] Y. Li, Y. Luo, R. Zhou, X. Zuo, Y. Zhang, Z. Wang, X. Li, X. Zhang, Z. Qin, C.S.K. Lin, Coculture of *Chlorella protothecoides* and *Coccomyxa subellipsoidea* enhances cell growth and lipid accumulation: an effective strategy for biodiesel production, *Chem. Eng. J.* 486 (2024) 150302.

[29] S. Ruangsomboon, P. Sornchai, N. Prachom, Enhanced hydrocarbon production and improved biodiesel qualities of *Botryococcus braunii* KMITL 5 by vitamins thiamine, biotin and cobalamin supplementation, *Algal Res.* 29 (2018) 159–169.

[30] J. Han, L. Zhang, S. Wang, G. Yang, L. Zhao, K. Pan, Co-culturing bacteria and microalgae in organic carbon containing medium, *J Biol Res (Thessalon)* 23 (2016) 8.

[31] R.M. Soo, B.J. Woodcroft, D.H. Parks, G.W. Tyson, P. Hugenholtz, Back from the dead: the curious tale of the predatory cyanobacterium *Vampirovibrio chlorellavorus*, *PeerJ* 3 (2015) e968.

[32] V. Serra, L. Gammuto, G. Petroni, A. Ciurli, C. Chiellini, Identification of the bacteria associated to the phycosphere of the *Chlorella*-like strain SEC_LI_ChL_1, *Algal Res.* 67 (2022) 102869.

[33] Y.-J. Sung, T. Takahashi, Y.-H. Lin, T.Z. Jia, Y.-R. Chiang, P.-H. Wang, Microalgal polyphosphate drives one-pot complete enzymatic generation of flavin adenine dinucleotide from adenosine and riboflavin, *ACS Sustain. Chem. Eng.* 12 (2024) 680–686.

[34] M. Fenech, Folate (vitamin B9) and vitamin B12 and their function in the maintenance of nuclear and mitochondrial genome integrity, *Mutat. Res.* 733 (2012) 21–33.

[35] T. Croft Martin, J. Warren Martin, G. Smith Alison, Algae need their vitamins, *Eukaryot. Cell* 5 (2006) 1175–1183.

[36] O.A. Palacios, Y. Bashan, L.E. de Bashan, Proven and potential involvement of vitamins in interactions of plants with plant growth-promoting bacteria—an overview, *Biol. Fertil. Soils* 50 (2014) 415–432.

[37] C. Nef, S. Jung, F. Mairet, R. Kaas, D. Grizeau, M. Garnier, How haptophytes microalgae mitigate vitamin B12 limitation, *Sci. Rep.* 9 (2019) 8417.

[38] K.P. Papadopoulos, M.F. de Souza, L. Archer, A.C.Z. Illanes, E.L. Harrison, F. Taylor, M.P. Davey, D.A. Gallardo, A.J. Komakech, S. Radmehr, A. Holzer, E. Meers, A.G. Smith, P. Mehrshahi, Vitamin B12 bioaccumulation in *Chlorella vulgaris* grown on food waste-derived anaerobic digestate, *Algal Res.* 75 (2023) 103290.

[39] S.A. Sañudo-Wilhelmy, C.J. Gobler, M. Okbamichael, G.T. Taylor, Regulation of phytoplankton dynamics by vitamin B12, *Geophys. Res. Lett.* 33 (2006) L04604.

[40] C. Panzeca, A. Tovar-Sánchez, S. Agustí, I. Reche, C.M. Duarte, G.T. Taylor, S. A. Sañudo-Wilhelmy, B vitamins as regulators of phytoplankton dynamics, *EOS Trans. Am. Geophys. Union* 87 (2006) 593–596.

[41] K. Skjånes, C. Rebours, P. Lindblad, Potential for green microalgae to produce hydrogen, pharmaceuticals and other high value products in a combined process, *Crit. Rev. Biotechnol.* 33 (2013) 172–215.

[42] R. Rautenberger, A. Détain, K. Skjånes, P.S.C. Schulze, V. Kiron, D. Morales-Sánchez, Growth strategies of *Chlorella vulgaris* in seawater for a high production of biomass and lipids suitable for biodiesel, *Algal Res.* 77 (2024) 103360.

[43] J.C. da Silva, A.T. Lombardi, Chlorophylls in microalgae: Occurrence, distribution, and biosynthesis, in: E. Jacob-Lopes, M.I. Queirozo, L.Q. Zepka (Eds.), *Pigments from Microalgae Handbook*, Springer International Publishing, Cham, 2020, pp. 1–18.

[44] P. Jakhwal, E. Daneshvar, K. Skalska, L. Matsakas, A. Patel, Y. Park, A. Bhatnagar, Nutrient removal and biomass production of marine microalgae cultured in recirculating aquaculture systems (RAS) water with low phosphate concentration, *J. Environ. Manag.* 358 (2024) 120859.

[45] S.A. Razzak, Comprehensive overview of microalgae-derived carotenoids and their applications in diverse industries, *Algal Res.* 78 (2024) 103422.

[46] M.-Y. Zhang, X.-R. Xu, R.-P. Zhao, C. Huang, Y.-D. Song, Z.-T. Zhao, Y.-B. Zhao, X.-J. Ren, X.-H. Zhao, Mechanism of enhanced microalgal biomass and lipid accumulation through symbiosis between a highly succinic acid-producing strain of *Escherichia coli* SUC and *Aurantiochytrium* sp. SW1, *Bioresour. Technol.* 394 (2024) 130232.

[47] Y. Kato, T. Oyama, K. Inokuma, C.J. Vavricka, M. Matsuda, R. Hidese, K. Satoh, Y. Oono, J.-S. Chang, T. Hasunuma, A. Kondo, Enhancing carbohydrate repartitioning into lipid and carotenoid by disruption of microalgae starch debranching enzyme, *Commun. Bio.* 4 (2021) 450.

[48] A.F. Esteves, E.M. Salgado, V.J.P. Vilar, A.L. Gonçalves, J.C.M. Pires, A growth phase analysis on the influence of light intensity on microalgal stress and potential biofuel production, *Energy Convers. Manag.* 311 (2024) 118511.

[49] T.-Y. Tsai, I. Khozin-Goldberg, A. Vonshak, T.-M. Lee, Ascorbate-glutathione cycle alleviates low-temperature-induced oxidative stress for augmented growth of *Nannochloropsis oceanica* rose Bengal mutants, *Physiol. Plant.* 176 (2024) e14168.

[50] J. Zhu, Y. Cai, M. Wakisaka, Z. Yang, Y. Yin, W. Fang, Y. Xu, T. Omura, R. Yu, A.L. Zheng, Mitigation of oxidative stress damage caused by abiotic stress to improve biomass yield of microalgae: a review, *Sci. Total Environ.* 896 (2023) 165200.

[51] Y.M. Zhang, H. Chen, C.L. He, Q. Wang, Nitrogen starvation induced oxidative stress in an oil-producing green alga *Chlorella sorokiniana* C3, *PLoS One* 8 (2013) e69225.

[52] M.C. Ruiz-Domínguez, I. Vaquero, V. Obregón, B. de la Morena, C. Vilchez, J. M. Vega, Lipid accumulation and antioxidant activity in the eukaryotic acidophilic microalga *Coccomyxa* sp. (strain *onubensis*) under nutrient starvation, *J. Appl. Phycol.* 27 (2015) 1099–1108.

[53] T.Q. Shi, L.R. Wang, Z.X. Zhang, X.M. Sun, H. Huang, Stresses as first-line tools for enhancing lipid and carotenoid production in microalgae, *Front. Bioeng. Biotechnol.* 8 (2020) 610.

[54] H. Alishah-Aratboni, N. Rafiei, R. Garcia-Granados, A. Alemzadeh, J.R. Morones-Ramirez, Biomass and lipid induction strategies in microalgae for biofuel production and other applications, *Microb. Cell Factories* 18 (2019) 178.

[55] D. Morales-Sánchez, P.S.C. Schulze, V. Kiron, R.H. Wijffels, Production of carbohydrates, lipids and polyunsaturated fatty acids (PUFA) by the polar marine microalga *Chlamydomonas malina* RCC2488, *Algal Res.* 50 (2020) 102016.

[56] D.H. Kim, H.S. Yun, Y.S. Kim, J.G. Kim, Effects of co-culture on improved productivity and bioresource for microalgal biomass using the floc-forming bacteria *Melaminivora Jejuensis*, *Front. Bioeng. Biotechnol.* 8 (2020) 588210.

[57] T. Yukino, M. Hayashi, I. Maruyama, H. Murata, Incorporation of exogenous docosahexaenoic acid into triacylglycerols and polar lipids of *Chlorella vulgaris*, *J. Oleo Sci.* 54 (2005) 15–19.

[58] N. Kato, G. Nelson, K.J. Laversen, Subcellular localizations of catalase and exogenously added fatty acid in *Chlamydomonas reinhardtii*, *Cells* 10 (2021).

[59] Y.K. Dasan, M.K. Lam, S. Yusup, J.W. Lim, P.L. Show, I.S. Tan, K.T. Lee, Cultivation of *Chlorella vulgaris* using sequential-flow bubble column photobioreactor: a stress-inducing strategy for lipid accumulation and carbon dioxide fixation, *J. CO₂ Util.* 41 (2020) 101226.

[60] H. Wang, X. Zhang, M. Gao, S. Gong, Y. Xu, J. Wang, M. Zhang, M. Xu, T. Zhao, Z. Zhang, Multi-omics insights of biotin-enhanced astaxanthin and total fatty acid productivity in heterotrophic *Chromochloris zofingiensis* under stress conditions, *Algal Res.* 90 (2025) 104158.

[61] H. Wang, X. Hu, C. Shao, M. Elshobary, F. Zhu, Y. Cui, C. Zhang, J. Ni, S. Huo, Optimizing mixotrophic cultivation of oil-rich *Tribonema minus* using volatile fatty acids and glycerin: a promising approach for pH-controlling and enhancing lipid productivity, *J. Clean. Prod.* 402 (2023) 136733.